International Journal of Biological Macromolecules 320 (2025) 145658

Contents lists available at ScienceDirect

International Journal of Biological Macromolecules

journal homepage: www.elsevier.com/locate/ijbiomac

Next-generation bioremediation: Molecular decoding of fungal laccases for efficient degradation of bisphenol a and its derivatives

Reyhaneh Kalhor [a], Mahdieh Ameri Shah Reza [a], Rahim Aali [b], Hoda Abolhasani [a], Mohammad Hossein Mokhtarian [c], Hourieh Kalhor [a,*]

[a] Cellular and Molecular Research Center, Qom University of Medical Sciences, Qom, Iran
[b] Research Center for Environmental Pollutants, Qom University of Medical Sciences, Qom, Iran
[c] Sana Institute for Avian Health and Diseases Research, Tehran, Iran

ARTICLE INFO

Keywords:
Bisphenol A
Environmental pollution
Laccase
Molecular docking
Molecular dynamic stimulations

ABSTRACT

Bisphenol A (BPA) and its derivatives are pervasive environmental pollutants and known to be toxic and anti-androgenic endocrine disruptors. Despite global regulatory efforts, the environmental persistence and bio-accumulation potential of BPA and its derivatives, remain critical challenges. This study aims to characterize the atomic-level interactions between bisphenol derivatives and Laccase (Lac) enzymes from various white-rot fungal species, by utilizing advanced computational approaches. Therefore, molecular docking and molecular dynamics simulation were performed by AutoDock Vina and GROMACS software, respectively. The molecular docking results indicated that Lac from *Botrytis aclada* exhibited the highest binding affinities for bisphenol A (BPA, −7.8 kcal/mol) and bisphenol S (BPS, −7.7 kcal/mol), while Lac from *Trametes hirsuta* showed an exceptional affinity for bisphenol AF (BPAF, −8.5 kcal/mol). Additionally, Lac from *Rigidoporus microporus* demonstrated strong binding with bisphenol E (BPE, −8.1 kcal/mol) and bisphenol F (BPF, −7.8 kcal/mol). Molecular dynamics simulations confirmed the stability of these complexes over 100 ns, with RMSD values below 0.45 nm and binding free energies ranging from −21.83 to −3.24 kJ/mol. These findings provide critical insights into the enzymatic degradation of bisphenol derivatives, establishing a robust framework for next-generation bioremediation strategies. However, further investigation through in vitro assessments is necessary to confirm these results.

1. Introduction

Bisphenols (BPs) are a group of chemical compounds related to diphenylmethane, characterized by two hydroxyphenyl groups linked by a methylene bridge [1]. Among these, Bisphenol A (BPA) is widely recognized. BPA is used as a key raw material for the manufacture of various products, including polycarbonate and epoxy resins commonly found in plastic water bottles, food packaging, dental fillings, and thermal papers, with global production exceeding 3.5 million tons annually [2,3]. Therefore, humans can be frequently exposed to BPA through skin absorption, inhalation, and ingestion. Prolonged and unavoidable exposure to even low doses of BPA can lead to various diseases and poor health, including respiratory [4], neurodegenerative [5], cancer [6], and cardiovascular [7] diseases. Also, BPA is classified as an endocrine-disrupting chemicals (EDCs). Moreover, BPA has a high affinity for estrogen receptors (ERα and β) while also inhibiting androgen action by binding to androgen receptors (AR). As a result, it can reduce fertility in both men and women, increase the risk of prostate and breast cancer, and cause premature puberty [8,9].

Regulatory restrictions on BPA usage have prompted industries to develop BPA analogs, such as BPAF, BPE, BPF, and BPS, as substitutes. However, these derivatives have been detected in food chains and human tissues, raising concerns about their environmental persistence, bioaccumulation, and toxicity. Addressing these challenges, innovative and sustainable remediation strategies are required to mitigate contamination of BPA and its derivatives [10]. Among these strategies, bioremediation — utilizing biological systems (like plants, bacteria, fungi, and yeast) to degrade pollutants — offers an eco-friendly, cost-effective alternative [11]. Enzymatic degradation is considered as one of the most effective methods of bioremediation, particularly for BPA remove from wastewater and other environments [2,12]. Laccase (Lac) is a highly significant enzyme that plays a crucial role in removing

* Corresponding author.
E-mail address: hkalhor@muq.ac.ir (H. Kalhor).

https://doi.org/10.1016/j.ijbiomac.2025.145658
Received 16 March 2025; Received in revised form 17 June 2025; Accepted 28 June 2025
Available online 5 July 2025

pollutants from polluted water and biodegrading EDCs [13–15]. Lac (EC.1.10.3.2) is a monomeric enzyme belonging to the member of the multicopper oxidase (MCO) family. So far, the structure of the Lac enzyme of several fungi, including *Trametes versicolor*, has been resolved. The enzyme consists of three sequentially arranged cupredoxin-like domains, which contribute to the stability and functionality of the enzyme. Also, this enzyme contains multiple copper ions, which are crucial for its catalytic activity including: Type 1 (T1) copper which is responsible for the blue color of the enzyme and mediates electron transfer from the substrate to the enzyme, Type 2 (T2), and Type 3 (T3) copper which form a trinuclear cluster that is essential for the reduction of oxygen to water. During catalysis, the T1 copper site receives electrons from substrate then they are transferred to the T2/T3 cluster, where molecular oxygen is reduced to water, completing the catalytic cycle. The active site of Lac enzyme is designed to accommodate various ligands, including phenolic compounds and arylamines [16]. Many species of white-rot fungi, bacteria, and plants produce the Lac enzyme, which is determined to have varying specificity across different organisms [17,18]. Several factors contribute to the specificity of the Lac enzyme including: specific amino acid residues in the active site, the conformation and size of the binding pocket, and the difference in redox potential between the T1 copper site and the ligands [16,19]. Moreover, bioremediation by Lac enzyme has significant advantages when compared to traditional methods such as chemical oxidation and physical adsorption [20–25]. This enzyme plays an essential role in the bioremediation process due to its high catalytic activity, specificity, environmental friendliness, and capability to function under mild conditions. Additionally, it can transform contaminants into less toxic substances and modify their properties, making them more easily degradable (Supplementary Table S1). Lac enzyme has also demonstrated promising results in breaking phenolic pollutants, such as BPA, in wastewater [14,16,19,26,27]. Dalel Daassi et al. investigated BPA degradation by Lac's *Coriolopsis gallica* using gas chromatography–mass spectrometry (GC–MS). They primarily yielded carboxylic acids, such as β-hydroxybutyric, tartaric, and pyroglutamic acids, which are less harmful than the parent compound [28].

Conventional experimental techniques for screening Lac enzymes capable of degrading bisphenols require labor-intensive procedures such as enzyme purification, activity measurements, and kinetic studies. These methods are not only time-consuming and costly but also require complex equipment [10,11,28,29]. On the other hand, researchers frequently employ computational approaches to investigate protein dynamics, including molecular flexibility, structural mobility, and conformational variations; moreover, these approaches can provide insights into the protein functional mechanisms. In addition, computational approaches can predict how well enzymes work and help choose the best ones before in vitro, reducing costs and time. Although they can't fully replace experimental methods, they are useful for finding high-performance Lac enzymes for pollutant degradation [30,31].

Current research disproportionately focuses on the Lac of *Trametes versicolo*r, neglecting the enormous biodiversity of other fungal Lac that may have better degradation capabilities [29]. Furthermore, the molecular mechanisms underlying Lac specificity toward emerging BPA substitutes (e.g. BPAF, BPE, BPF, BPS) — which are increasingly replacing BPA in industrial applications — remain poorly understood [10]. Anther limitation of previous studies is their inability to predict the structure-activity relationships that determine the efficacy of Lac enzymes with different bisphenol compounds [28,32].

Despite the potential of Lac enzymes, the molecular mechanisms governing their interactions with BPA derivatives are unknown. Identifying effective Lac enzymes to degrade these derivatives is therefore critical. Thus, in this study, we employed advanced computational methods, including molecular docking and molecular dynamics simulations, to investigate the interactions between Lac enzymes from thirteen fungal species and bisphenol derivatives (e.g. BPAF, BPE, BPF, BPS). Unlike most previous studies, which have primarily focused on a single fungal species (typically *Trametes versicolor*) and bisphenol A (BPA), our approach provides a broader comparative analysis. Our findings reveal that Lac from *Botrytis aclada*, *Trametes hirsuta*, and *Rigidoporus microporus* exhibit the highest binding affinities and stability with BPA and its derivatives. These results provide critical insights into the enzymatic degradation mechanisms of bisphenols, establishing a robust theoretical foundation for optimizing Lac-based bioremediation strategies. This research represents a significant step toward developing scalable and sustainable solutions to mitigate the environmental and health impacts of bisphenol contamination.

2. Materials and method

2.1. Sequence analysis

The amino acid sequences of Lac enzyme from several fungi including *Trametes trogii*, *Trametes hirsuta*, *Coriolopsis gallica*, *Melanocarpus albomyces*, *Steccherinum ochraceum*, *Basidiomycete PM1*, *Trametes versicolor*, *Cerrena maxima*, *Rigidoporus microporus*, *Coprinopsis cinerea*, *Trametes coccinea*, *Botrytis aclada*, and *Canariomyces arenarius* were obtained from the UniProt database (http://www.uniprot.org/). Afterward, multiple sequence alignment (MSA) was performed to analyze of the T1, T2, and T3 copper-binding sites, by using the T-Coffee web server (https://tcoffee.crg.eu/apps/tcoffee/do:expresso).

2.2. Molecular docking

2.2.1. Preparation and selection receptors

The 3D crystal structures of selected Lac enzymes were obtained from the protein data bank (www.rcsb.org). In order to perform molecular docking, the selected PDB structures were processed using AutoDock Tools 4. This involved assigning bond orders, adjusting atom types, removing water molecules, and adding hydrogen atoms and Gasteiger-Marsili charges [33]. Lastly, 3D structures were saved in the PDBQT format as a receptor for molecular docking [34,35]. Based on literature information and crystallographic structures, the active sites of receptors, Lac enzymes, were identified. Specifically, residues involved in the T1 and T2 copper-binding sites were selected as reference residues for molecular docking [17,36–38]. Then, AutoDock Tools 4 was used to determine the grid box for the active sites of selected Lac enzymes.

2.2.2. Ligand preparation

The 2D structure of bisphenol compounds (BPA, BPAF, BPE, BPF, and BPS) were downloaded from the PubChem database (https://pubchem.ncbi.nlm.nih.gov/) as ligands and saved in SDF format. The ligands' 2D structures were then energetically minimized using chem3D software (version 17.1), employing both the minimized energy and molecular dynamics features using the MM2 force field. After that, the Optimized ligands were converted to SDF format using Open Babel software [39] for molecular docking.

2.2.3. Molecular docking study

We was performed flexible docking using the AutoDock Vina program [40]. The results of the docking and the molecular interactions between Lac enzymes and ligands were subsequently evaluated and visualized using Pymol and Discovery Studio software [41,42].

2.3. Physicochemical and toxicity analysis of the selected BP compounds

In this step, the physicochemical properties and toxicity of the selected BPs were evaluated. Key physicochemical properties, including molecular weight (MW), the logarithm of the partition coefficient (cLogP), the number of hydrogen bond donors (HBD) and hydrogen bond acceptors (HBA), as well as the polar surface area (PSA) and the number of rotatable bonds (RB) were obtained from the PubChem database. Also, Toxicological parameters such as mutagenicity (MUT),

tumorigenicity (TUM), irritant potential (IRR), and reproductive toxicity (RPE) were predicted using OSIRIS DataWarrior software [43].

2.4. Molecular dynamic simulations (MDs)

The structure stability of Lac/BP complexes was assessed using MDs conducted with GROMACS software. Topology files and force field parameters for BP compounds were generated using SwissParam [44], while receptor topology files were prepared using pdb2gmx with the CHARMM force field. The complexes were solvated in a simple point charge (SPC) water box with a 10 Å margin and neutralized using counterions (Na + or Cl−). Energy minimization was performed iteratively, followed by equilibration using the constant number of particles, volume, and temperature (NVT) and constant number of particles, pressure, and temperature (NPT) conditions for 500 ps at 300 K. Production simulations were conducted for 100 ns with a 2 fs time step. Trajectories were analyzed for further analysis.

2.5. Binding free energy analysis

The Molecular Mechanics/Poisson–Boltzmann Surface Area (MM/PBSA) method was used to evaluate the binding free energies of receptor-ligand complexes [45]. The energy components were decomposed into van der Waals interaction energy (ΔE_{vdW}), electrostatic interaction energy (ΔE_{ele}), polar solvation energy (ΔG_{PB}, calculated by the Poisson-Boltzmann equation), and nonpolar solvation energy (ΔG_{SA}, derived from the solvent-accessible surface area). Also, the gas-phase interaction energy (ΔE_{gas}), solvation-free energy (ΔG_{solv}), and total binding free energy (ΔG_{bind}) were calculated. However, the ΔG_{bind} was derived from the sum of ΔE_{gas} ($\Delta E_{vdW} + \Delta E_{ele}$) and ΔG_{solv} ($\Delta G_{PB} + \Delta G_{SA}$). These calculations were performed using snapshots extracted from the last 50 ns of MD trajectories at a sampling interval of 2 ps.

3. Results

3.1. Identification of conserved regions in the active centers of Lac enzymes

The amino acid sequences of thirteen fungi Lac enzymes were analyzed to investigate conserved residues in their active centers, specifically within the T1, T2, and T3 copper-binding sites, which are critical for catalytic function (Supplementary Fig. S1). Previous studies have identified key residues in the active center of Lac's *Trametes versicolor* include: Phe162, Pro163, Asp206, Pro207, Asn208, Asn264, Phe265, Ala393, and His458 residues in the T1 site and Ala80, Ser110, Ser113, Tyr116, His454, and Ile455 residues in the T2 site. Also, the T3 site includes Gln102, Asp224, Leu399, His402, and Asp424 residues [15,17,36,37]. The residues in these sites from *Trametes versicolor* were compared with other selected Lac enzymes. Comparative analysis revealed that the Phe162, Phe265, and Ala393 residues of *Trametes versicolor* were not conserved in the Lac enzymes of other fungi, whereas His454, Asn208, and Pro207 of *Trametes versicolor* were highly conserved. However, Pro207 and Asn208 of *Trametes versicolor* were not conserved in *Melanocarpus albomyces* (Asn286, His287), *Canariomyces arenarius* (Asn237, His238), and *Botrytis aclada* (Ser237, His238). Residues in the T2 and T3 sites were predominantly conserved, highlighting their critical roles in stabilizing the copper centers and maintaining enzymatic redox activity. Additionally, structural variations in the hydrophobic pocket of the T1 site, a region essential for substrate binding and catalytic function, were observed among species. These variations may influence substrate specificity and enzymatic efficiency. On the other hand, several studies have reported that the hydrophobic pocket of the T1 site plays a significant role in lignin degradation (Fig. 1).

Based on crystallographic data and sequence alignment, we identified the T1 site residues included Phe162, Pro163, Cys205, Asp206, Pro207, Asn208, Asn264, Phe265, Gly392, Ala393, and His458. as Also, we identified the T2 site residues comprised His454, Ile455, Asp456, and Phe457. These residues were selected as the key active site residues for molecular docking with BP compounds for all selected fungal Lac enzymes. More details of the active site of selected Lac enzymes are tabulated in Table 1.

3.2. Binding affinity analysis of Lac enzymes with BP compounds

Molecular docking is an important technique for determining optimal intermolecular interactions between proteins and ligands. This method is used to predict the best orientation, conformation, and binding affinity of a ligand at the binding site of a protein to finally determine the most stable ligand-protein complex based on a computational assessment [46]. In this study, molecular docking was performed between the active site of selected Lac enzymes and BP compounds using AutoDock Vina. The results indicated that the Lac

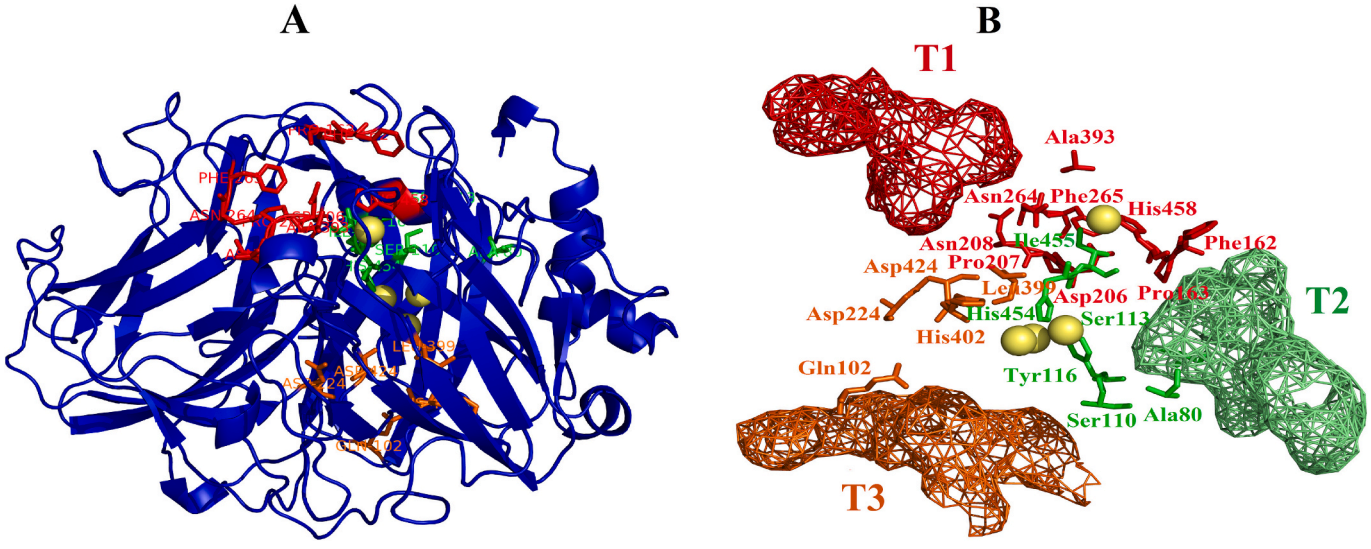

Fig. 1. (A) Cartoon representation of Lac's *Trametes versicolor* (blue) (PDB ID: 1KYA). (B) Mesh representation of the T1 (red color), T2 (green color), and T3 (orange color) copper-binding sites. Residues involved in the T1, T2, and T3 copper-binding sites of *Trametes versicolor* are shown as red, green, and orange sticks, respectively, also copper ions are shown as gold spheres.

Table 1
Details of selected fungal Lac enzymes and evaluation of residues in the active site, as well as the grid box for molecular docking.

NO	name	Uniport ID	PDB ID	Residue involve in the active site	Grid box
1	*Trametes trogii*	Q9HDQ0	2HRH	Val162, Pro163, Cys204, Asp205, Pro206, Asn207, Asn263, Ser264, Gly391, Phe392, His451, Ile452, Asp453, Phe454, His455	center_x = −5.897 center_y = −16.07 center_z = −16.887 size_x = 24 size_y = 24 size_z = 24
2	*Trametes hirsuta*	B2L9C1	3PXL	Phe162 Pro163, Cys205, Asn206, Pro207, Asn208, Asn264, Phe265, Gly392, Ala393, His454, Ile455, Asp456, Phe457, His458	center_x = 5.622 center_y = 18.721 center_z = 22.885 size_x = 24 size_y = 24 size_z = 24
3	*Coriolopsis gallica*	Q1W6B1	4A2D	Val183, Pro184, Cyc225, Asp226, Pro227, Asn284, Ser285, Gly412, Phe413, His472, Ile473, Asp474, Phe475, His476	center_x = 13.455 center_y = −16.66 center_z = −32.207 size_x = 24 size_y = 24 size_z = 24
4	*Melanocarpus albomyces*	Q70KY3	3FU7	Ala191, Pro193, Thr234, Glu235, Phe292, Gly293, Ser428, Leu429, Ile505, Ala506, Trp507, His508	center_x = −17.917 center_y = 31.303 center_z = 26.643 size_x = 24 size_y = 24 size_z = 24
5	*Steccherinum ochraceum*	I13B14	3T6V	Gly164, Ala165, Cys208, Asp209, Pro210, Asn211, Asn267, Ser268, Gly394, Gly395, His454, Ile455, Asp456, Trp457, His458	center_x = 22.339 center_y = −19.871 center_z = −27.702 size_x = 24 size_y = 24 size_z = 24
6	*Basidiomycete PM1*	Q12571	5ANH	Val162, Pro163, Cys204, Asp205, Pro206, Asn207, Asn263, Ser264, Gly391, Phe392, His451, Ile452, Asp453, Phe454, His455	center_x = 20.604 center_y = −3.369 center_z = 24.338 size_x = 24 size_y = 24 size_z = 24
7	*Trametes versicolor*	Q96UT7	1KYA	PHE162, Pro163, Cys205, ASP 206, PRO207, ASN208, ASN264, PHE265, Gly392, ALA393, HIS454, ILE455, ASP456, PHE457, HIS458	center_x = −25.868 center_y = 7.3318 center_z = 57.138 size_x = 24 size_y = 24 size_z = 24
8	*Cerrena maxima*	D0VWU3	3DIV	Phe162, Pro163, Cys205, Asp206, Pro207, Asn208, Asn264, Phe265, Gly392, Ala393, His454, Ile455, Asp456, Phe457, His458	center_x = 5.626 center_y = 54.43 center_z = 24.321 size_x = 24 size_y = 24 size_z = 24
9	*Rigidoporus microporus*	Q6H9H7	1V10	Ala166, Peo167, Cys210, Phe211, Pro212, Asn213, Ser269, Asn270, Gly394, His453, Ile454, Asp455, Trp456, His457	center_x = −13.961 center_y = 82.336 center_z = −11.147 size_x = 24 size_y = 24 size_z = 24
10	*Coprinopsis cinerea*	Q9Y780	1HFU	Cys204, Asp205, Asn263, Lys264, Gly393, Gly394, Ile454, Glu455, Phe456, His457	center_x = 25.499 center_y = 29.635 center_z = 42.218 size_x = 24 size_y = 24 size_z = 24
11	*Trametes coccinea*	Q96TR6	5NQ7	Phe183, Pro184, Cys226, Asp227, Pro228, Asn229, Pro285, Phe286, Gly413, Ser414, His473, Ile474, Asp475, Phe476, His477	center_x = 82.377 center_y = 34.414 center_z = 39.699 size_x = 24 size_y = 24 size_z = 24
12	*Botrytis aclada*	H8ZRU2	3SQR	Ala184, Pro185, Ile235, Asp236, Ser237, His238, Gly294, Gly423, Ile424, His490, Ile491, Ala492, Trp493, His494	center_x = 3.645 center_y = −2.27 center_z = −9.677 size_x =

(*continued on next page*)

Table 1 (*continued*)

NO	name	Uniport ID	PDB ID	Residue involve in the active site	Grid box
13	*Canariomyces arenarius*	F6N9E7	3PPS	Gly192, Ala193, Thr235, Asp236, Asn237, His238, Gly294, Ser429, Leu430, His505, Ile506, Ala507, Trp508, His509	24 size_y = 24 size_z = 24 center_x = 18.966 center_y = −10.352 center_z = 0.312 size_x = 24 size_y = 24 size_z = 24

enzyme from *Trametes hirsuta* has the highest binding affinity with BPAF, −8.5 kcal/mol. Moreover, *Rigidoporus microporus* Lac displayed notable binding affinity with BPE and BPF, achieving maximum values of −8.1 and − 7.8 kcal/mol, respectively. Lac's *Botrytis aclada* demonstrated strong binding affinity with BPA and BPS, with values of −7.8 and − 7.7 kcal/mol, respectively. The Lac enzymes of *Trametes versicolor*, *Cerrena maxima*, and *Trametes coccinea* displayed a higher binding affinity for BPA than BPAF, BPE, BPF, and BPS with a value of −7.5, −7.2, and − 7.2 kcal/mol, respectively. Also, the Lac enzymes of *Steccherinum ochraceum*, *Coprinus cinerea*, and *Canariomyces arenarius* exhibited higher binding affinity with BPE compared to BPA, BPAF, BPF, and BPS with values of −7.3, −7.5, and − 7.5 kcal/mol, respectively. Furthermore, the Lac enzymes of *Trametes trogii* and *Coriolopsis gallica* exhibited a stronger affinity for BPF compared to BPA, BPAF, BPE, and BPS, with binding values of −7.2 and − 7.5 kcal/mol, respectively. While the Lac enzymes of *Basidiomycete PM1* and *Botrytis aclada* exhibited a stronger affinity for BPS compared to BPA, BPAF, BPE, and BPF with binding values of −7.4 and − 7.7 kcal/mol, respectively. The detailed results of the binding affinity for each complex are presented in Table 2. It can see Table 2, the Lac enzymes from *Trametes trogii* and *Melanocarpus albomyces* exhibited the lowest binding affinity with BPA, BPAF, BPE, BPF, and BPS compounds (binding affinity range: −5.7 to −6.8 kcal/mol). Specifically, the Lac enzymes from *Trametes trogii* displayed a higher binding affinity BPF than with other BP compounds (−7.2 kcal/mol). Our analysis showed that the Lac enzymes from *Trametes hirsuta*, *Rigidoporus microporus*, and *Botrytis aclada* exhibited the highest binding affinities (−8.5 to −7.1 kcal/mol) and the most favorable conformations with the bisphenols BPA, BPAF, BPE, BPF, and BPS, in comparison to other Lac enzymes. Consequently, these Lac enzyme complexes with the mentioned bisphenols were chosen for further analysis.

Table 2
Evaluation of binding affinity of selected fungal Lac enzymes to BP compounds.

NO	name	Binding affinity (Kcal/mol)				
		BPA	BPAF	BPE	BPF	BPS
1	*Trametes trogii*	−5.7	−5.7	−6.5	−7.2	−6.8
2	*Trametes hirsuta*	−7.1	−8.5	−7.1	−7.3	−6.8
3	*Coriolopsis gallica*	−6.2	−6.9	−7.0	−7.5	−7.0
4	*Melanocarpus albomyces*	−6.6	−6.8	−6.8	−6.4	−6.4
5	*Steccherinum ochraceum*	−6.8	−6.8	−7.3	−7.1	−7.0
6	*Basidiomycete PM1*	−6.6	−6.8	−7.0	−7.3	−7.4
7	*Trametes versicolor*	−7.5	−6.8	−6.8	−6.7	−7.3
8	*Cerrena maxima*	−7.2	−6.5	−7.0	−6.7	−6.8
9	*Rigidoporus microporus*	−7.2	−7.5	−8.1	−7.8	−7.3
10	*Coprinopsis cinerea*	−6.8	−6.7	−7.5	−7.3	−7.2
11	*Trametes coccinea*	−7.2	−6.7	−6.1	−6.8	−6.0
12	*Botrytis aclada*	−7.8	−7.3	−7.5	−7.4	−7.7
13	*Canariomyces arenarius*	−7.1	−5.7	−7.5	−7.2	−6.6

3.3. Molecular interactions between selected fungal Lac enzymes and BP compounds

The analysis of molecular interactions between selected Lac and BP compounds revealed that Lac's *Trametes hirsuta* interacts with BPA in the following ways: one conventional hydrogen bond with Asn264; four van der Waals bonds with Pro391, Gly392, Ala393, and Pro394; a pi-sigma bond with Phe265 with binding affinity −7.1 kcal/mol. This enzyme interacts with BPAF through one conventional hydrogen bond with Gly392; one van der Waals bond with Asn264; one pi-alkyl bond with Phe265, and one halogen (fluorine) bond with Ala393 and binding affinity −8.5 kcal/mol. As for BPE, it interacts through one conventional hydrogen bond with Asn264 along with four van der Waals bonds with Gly164, Gly392, Ala393, and Pro394, a pi-sigma bond with Phe265 with binding affinity −7.1 kcal/mol. This enzyme interacts with BPF through one conventional hydrogen bond with Gly392 and also forms seven van der Waals bonds with Gly164, Asn206, Asn264, Ala393, Pro394, Ile455, and His458 as well as a pi-alkyl bond with Phe265. The binding affinity in this case is −7.3 kcal/mol. While BPS interacts with Lac's *Trametes hirsuta* through two conventional hydrogen bonds with Gly392 and Ala393; three van der Waals bonds with Gly164, Asn264, and Phe265; a carbon-hydrogen bond with Pro391 and its binding affinity is −6.8 kcal/mol (Figs. 2, 3, 4, Table 2, and Table 3).

The Lac's *Rigidoporus microporus* interacts with BPA through van der Waals and pi-alkyl bonds. It forms five van der Waals bonds with Ala166, Arg336, Gly394, Ile454, and His457 as well as one pi-alkyl bond with Phe211. The binding affinity between this enzyme and BPA is −7.2 kcal/mol. Furthermore, this enzyme interacts with BPAF through six van der Waals bonds with Ala166, Phe211, Arg336, Asn395, and Ile454. It also forms one pi-alkyl bond with His457 and two halogen (fluorine) bonds with Gly394 with a binding affinity of −7.5 kcal/mol. In addition, BPE interacts with the enzyme through conventional hydrogen bonds and van der Waals bonds. It forms three conventional hydrogen bonds with Asn213, Ser269, and Arg336, as well as seven van der Waals bonds with Phe211, Pro212, Gly394, Asn395, Pro397, Ile454, and His457. The binding affinity between BPE and the enzyme is −8.1 kcal/mol. Also, this enzyme interacts with BPF through two conventional hydrogen bonds with Asn213 and Arg336. It also forms six van der Waals bonds with Phe211, Ser269, Gly394, Asn395, Ile454, and His457. The binding affinity between BPF and this enzyme is −7.8 kcal/mol. BPS interacts with this enzyme through conventional hydrogen bonds with Asn270 and Arg336. It forms three van der Waals bonds with Ala166, Ile454, and His457, as well as one pi-sulfur bond with Phe211. The binding affinity between BPS and the enzyme is −7.3 kcal/mol (Figs. 2, 3, 4, Table 2, and Table 3).

The Lac's *Botrytis aclada* interacts with BPA in several ways. Firstly, it forms a conventional hydrogen bond with Cys297. Additionally, it forms eight van der Waals bonds with Gly183, Ala184, Thr296, Ser298, Thr299, Phe365, Trp367, and Phe422. It also forms two pi-alkyl bonds with Pro185 and Ile424. Finally, it forms a pi-donor hydrogen bond with Phe422. The binding free energy for this interaction is −7.8 kcal/mol.

This enzyme also interacts with BPAF. In this case, it forms a halogen bond with Gly183 and three van der Waals bonds with Ser298, Trp367, and Ile424. It also forms three pi-alkyl bonds with Ala184, Phe365, and Phe422. The binding affinity for this interaction is −7.3 kcal/mol.

BPE interacts with the enzyme through two conventional hydrogen bonds with Gly183 and Cys297. Additionally, it forms five van der Waals bonds with Ala184, Thr299, Trp367, Ile424, and His494 with Ser298 residues. It also forms a pi-donor hydrogen bond with Ser298 and two pi-alkyl bonds with Pro185 and Phe422. The binding affinity for this interaction is −7.5 kcal/mol. For the interaction with BPF, this enzyme forms five van der Waals bonds with Gly183, Cys297, Thr299, Phe365, and Trp367. It also forms three pi-alkyl bonds with Ala184, Pro185, and

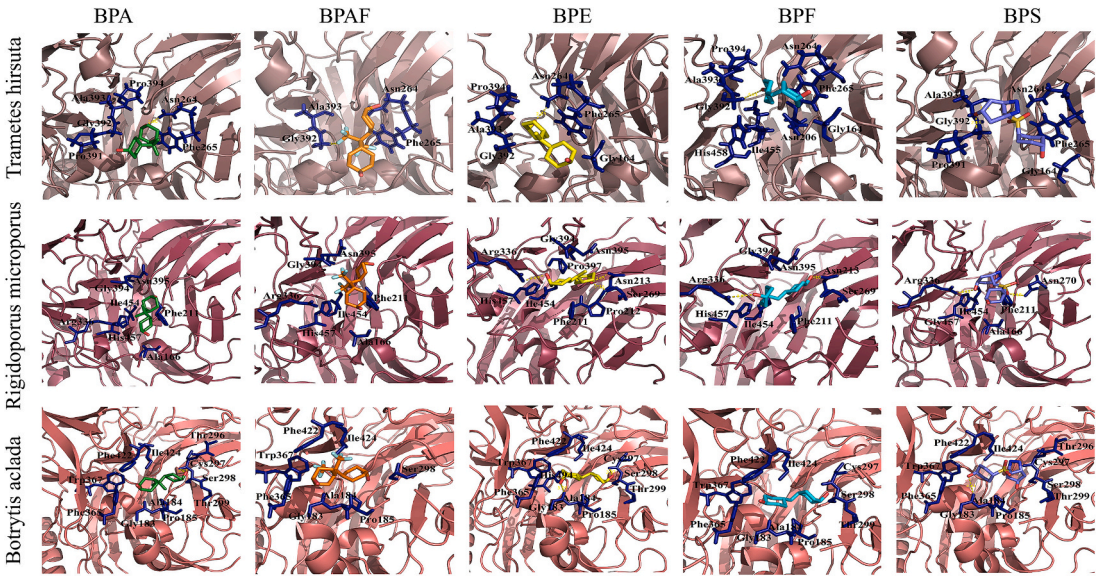

Fig. 2. Three-dimensional structure illustration of interactions between selected Lac enzymes from fungi and BP compounds with the highest affinity. The 3D structure of Lac's *Trametes hirsuta* (ruby), Lac's *Rigidoporus microporus* (raspberry), and Lac's *Botrytis aclada* (deepsalmon) in complexes are shown in cartoon representation. The deep blue stick represents residues involved in interactions. Also, the Hydrogen bonds in the complexes are shown as yellow dotted lines. The 3D illustrates BPA, BPAF, BPE, BPF, and BPS are colored green, orange, yellow, cyan, and blue, respectively with stick representation in the complexes.

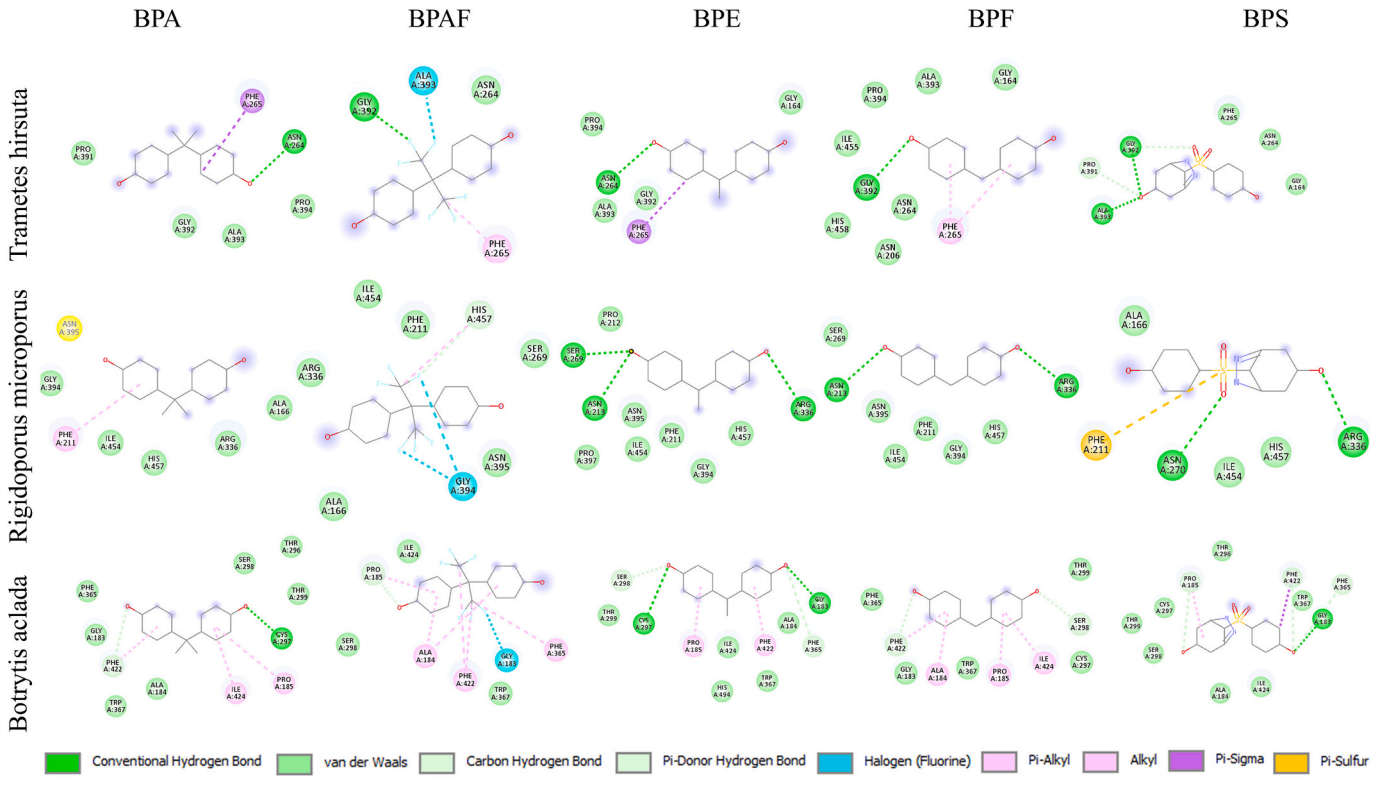

Fig. 3. The two-dimensional structure illustrates interactions between selected Lac enzymes from fungi and BP compounds with the highest affinity.

Ile424. Additionally, it forms a pi-donor hydrogen bond with Ser298 and a carbon-hydrogen bond with Phe422. The binding affinity for this interaction is −7.4 kcal/mol. Moreover, this enzyme interacts with BPS through a conventional hydrogen bond with Gly183. It also forms seven van der Waals bonds with Ala184, Thr296, Cys297, Ser298, Thr299, Trp367, and Ile424. Additionally, it forms three pi-donor hydrogen bonds with Pro185, Phe365, and Phe422. The binding affinity for this interaction is −7.7 kcal/mol (Figs. 2, 3, 4, Table 2, and Table 3).

Detailed interaction analyses revealed critical insights into the binding mechanisms of high affinity Lac/BP complexes for example: in Lac's *Trametes hirsute*/BPAF complex, Lac's *Rigidoporus microporus*/BPE and BPF complexes, and Lac's *Botrytis aclada*/BPA and BPS complexes showed strong interactions.

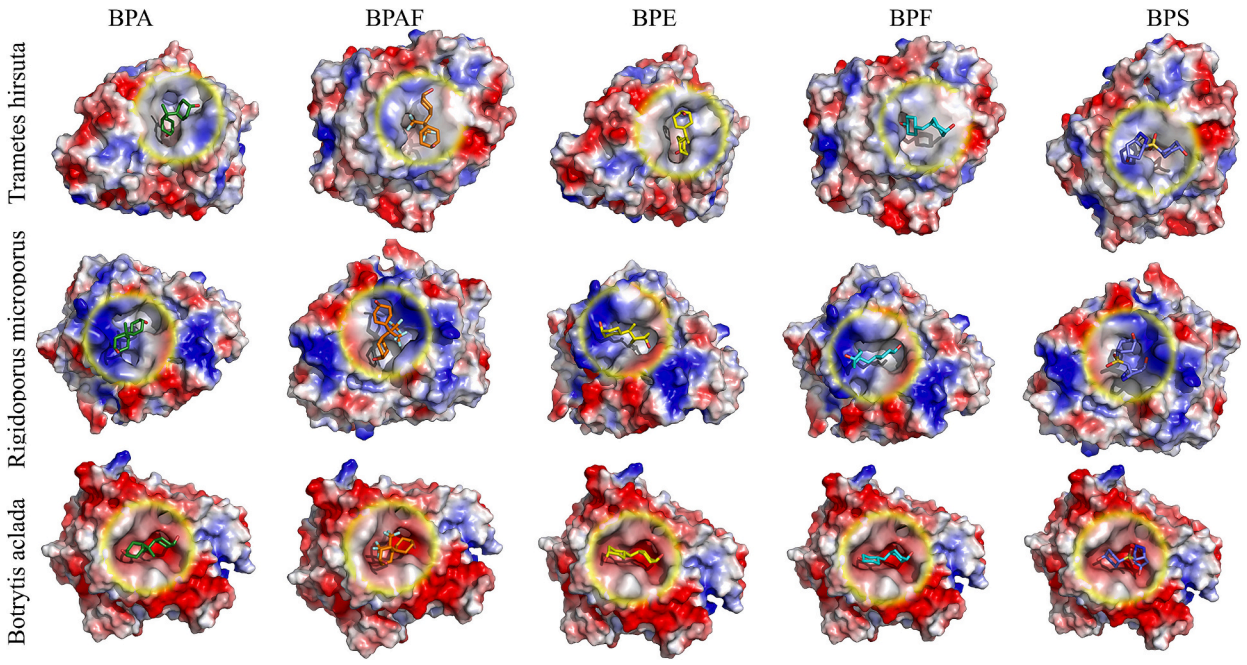

Fig. 4. Electrostatic potential surface representation of selected Lac enzymes from fungi docked with selected BP compounds with the highest affinity. The 3D illustration of BPA, BPAF, BPE, BPF, and BPS are colored green, orange, yellow, cyan, and blue, respectively with stick representation in the complexes. Blue Positive regions, red negative regions, and white hydrophobic regions. The binding site of selected BP compounds to selected Lac enzymes is shown with an open yellow circle.

3.4. Evaluation of the physicochemical properties and toxicity risk parameters of the selected BP compounds

The analysis of key physicochemical properties and toxicity risk parameters for the selected BP compounds revealed the following results: MW ranged from 200.23 to 336.23 g/mol, calculated cLogP ranged from 1.0 to 4.5, HBA and HBD were 2, PSA was 40.5, RBs were 2. Notably, BPAF had an HBA of 8, and BPS had a PSA of 80.3. Toxicity calculations indicated that BPA exhibited high toxic behaviors, whereas BPAF, BPE, and BPS had primarily high IRR. Interestingly, BPF showed no toxic behaviors. Detailed calculations of these parameters for the selected BP compounds are presented in Table 4.

3.5. Evaluation of the complex's structures during MD simulation

MD simulation is a powerful computational method for studying the dynamic behavior of protein-ligand complexes and their interactions at the atomic level [47–50]. In this study, MD simulations were performed on protein structures, focusing on the complexes, with the strongest binding affinity and the best conformations, the Lac's *Botrytis aclada* with BPA and BPS, the Lac's *Trametes hirsuta* with BPAF, and the Lac's *Rigidoporus microporus* with BPE and BPF. The RMSD value is a quantitative measure of the conformational changes in the protein structure. The RMSD of the complexes was calculated by considering the protein backbone throughout the 100 ns simulation. The RMSD value for the complex of Lac's *Botrytis aclada* with BPA fluctuated in the range of 0.10 to 0.44 nm in the first 45 ns and reached a stable value of ~0.38 nm from 45 ns to the end of the simulation. The RMSD value for the complex of Lac's *Trametes hirsuta* with BPAF fluctuated between 0.05 and 0.22 nm and reached its steady state at 0.15 nm between 5 ns and 38 ns then increased slightly and remained at ~0.19 nm from 40 ns till the end of the simulation.

The RMSD value for the complex of Lac's *Rigidoporus microporus* with BPE fluctuated in the range of about 0.05 to 0.28 nm and reached its steady state at ~0.22 nm from 10 ns to 70 ns. Then it slightly increased and persisted at ~0.24 m from 70 ns till the end of the simulation. This value for the complex of Lac's *Rigidoporus microporus* with BPF also fluctuated in the range of about 0.05 to 0.28 nm; however, it remained stable at ~0.20 nm from 15 ns till the end of the simulation, except between 57 ns and 62 ns timescale. The RMSD value for the complex of Lac's *Botrytis aclada* with BPS fluctuated from 0.01 to 0.22 nm between 3 ns and 70 ns and reached its steady state at 0.18 nm, then increased slightly and remained stable at ~0.25 nm from 70 ns till the end of the simulation (Fig. 5A).

The Rg value was calculated as an indicator of stability and also protein structure compactness. As depicted in Fig. 5B, the complex of Lac's *Botrytis aclada* with BPA fluctuated from 2.25 to 2.35 nm between 20 ns and 45 ns, then increased slightly and remained stable at ~2.33 nm from 45 ns till the end of the simulation. The Rg value of Lac's *Trametes hirsuta* with BPAF was stable at ~2.22 nm during 100 ns simulation, except between 40 ns and 50 ns. This value for Lac's *Rigidoporus microporus* with BPE and BPF was stable at ~2.18 nm and ~ 2.2 nm, respectively, throughout the simulation. The Rg value of the complex of Lac's *Botrytis aclada* with BPS was stable at ~2.26 nm in the first 60 ns, then increased slightly and remained stable at ~2.28 nm from 60 ns till the end of the simulation.

Hydrogen bonds are essential for the binding and stability of protein-ligands. We examined the number of hydrogen bonds between protein and ligand in complexes during 100 ns MDs. The results of the numbers of hydrogen bonds (H-bonds) showed that the complex of Lac's *Botrytis aclada* with BPA and Lac's *Trametes hirsuta* with BPAF possessed 0–3H-bonds, Lac's *Rigidoporus microporus* with BPE and *Botrytis aclada* with BPS had 0–4H-bonds, and the Lac's *Rigidoporus microporus* with BPF had 0–1H-bonds. In general, all complexes had an average of two H-bonds, which were very stable throughout MD simulations, except for the complex of Lac's *Rigidoporus microporus* with BPF (Fig. 5C).

The RMSF value was computed from the trajectories of each complex to evaluate the flexibility of each residue. Generally, lower RMSF values indicate greater rigidity, while higher RMSF values indicate increased flexibility (Fig. 5D). The RMSF plot for the complex of Lac's *Botrytis aclada* with BPA and BPS uncovered that 1–543 residues fluctuated between 0.04 nm and 1.40 nm, and 0.03 nm and 0.51 nm, respectively.

Table 3
Evaluation interacting residues in the Lac/BP compound complexes.

BP compounds	*Trametes hirsuta*		*Rigidoporus microporus*		*Botrytis aclada*	
	HB-AA, distance	NH-AA	HB-AA, distance	NH-AA	HB-AA, distance	NH-AA
BPA	Asn264, N-H…O=C; 2.90 Å	Phe265, Pro391, Gly392, Ala393, Pro394	—	Ala166, Arg336, Gly394, Ile454, His457, Phe211	Cys297, C=O···O=C; 3.27 Å	Gly183, Ala184, Thr296, Ser298, Thr299, Phe365, Trp367, Phe422, Pro185, Ile424
BPAF	Gly392, C-H···F-C; 2.57 Å	Asn264, Phe265, Ala393	—	Ala166, Phe211, Arg336, Gly394, Asn395, Ile454, His457,	—	Gly183, Ala184, Ser298, Trp367, Phe365, Phe422, Ile424
BPE	Asn264, C-H…O=C; 2.93 Å	Gly164, Phe265, Gly392, Ala393, Pro394	Asn213, C=O···O=C; 3.95 Å Ser269, C=O···O=C; 2.70 Å Arg336, N-H…O=C; 3.23 Å	Phe211, Pro212, Gly394, Asn395, Pro397, Ile454, His457	Gly183, C=O···O=C; 3.09 Å Cys297, C=O···O=C;3.37 Å	Ala184, Pro185, Ser298, Thr299, Trp367, Ile424, His494, Phe422
BPF	Gly392, C-H…O=C; 4.21 Å	Gly164, Asn206, Asn264, Phe265, Ala393, Pro394, Ile455, His458	Asn213, C=O···O=C; 3.18 Å Arg336, N-H…O=C; 3.07 Å	Phe211, Ser269, Gly394, Asn395, Ile454, His457	—	Gly183, Ala184, Pro185, Cys297, Thr299, Phe365, Trp367, Ile424
BPS	Gly392, C-H… O=C;2.16 Å Ala393, C=O···O=C; 3.70 Å	Gly164, Asn264, Phe265, Pro391	Asn270, N-H…O=C; 3.18 Å Arg336, N-H…O=C; 3.11 Å	Ala166, Ile454, His457, Phe211	Gly183, C=O···O=C; 331 Å	Ala184, Thr296, Cys297, Ser298, Thr299, Trp367, Ile424, Pro185, Phe365, Phe422

Table 4
Evaluation of physicochemical properties of selected BP compounds using OSIRIS Data Warrior.

Name compound	Physicochemical properties								Toxicity risks parameters			
	PubID[a]	MF[b]	MW[c]	CLP[d]	HBA[e]	HBD[f]	PSA[g]	RB[h]	MUT[i]	TMU[j]	IRR[k]	RPE[l]
BPA	6623	C15H16O2	228.29	3.3	2	2	40.5	2	High	High	High	High
BPAF	73,864	C15H10F6O2	336.23	4.5	8	2	40.5	2	No	No	High	No
BPE	608,116	C14H14O2	214.26	3.9	2	2	40.5	2	No	No	High	Low
BPF	12,111	C13H12O2	200.23	2.4	2	2	40.5	2	No	No	No	No
BPS	6626	C12H10O4S	250.27	1.9	2	2	80.3	2	No	No	High	No

[a] PubChemCID.
[b] MolecularFormula.
[c] Molecular weight (g/mol).
[d] cLogP(lipophilicity).
[e] H-bond acceptors.
[f] H-bond donors.
[g] Polar Surface Area(A^2).
[h] Rotatable bonds.
[i] MUT, mutagenic.
[j] TUM, tumorigenic.
[k] IRR, irritant.
[l] RPE, reproductive effective.

The RMSF plot in the complexes of Lac's *Trametes hirsuta* with BPAF residues 1–503 fluctuated between 0.04 nm and 0.30 nm. This plot in Lac's *Rigidoporus microporus* with BPE and BPF (residues 1–491) fluctuated between 0.03 nm and 0.53 nm, and 0.03 nm and 0.51 nm, respectively.

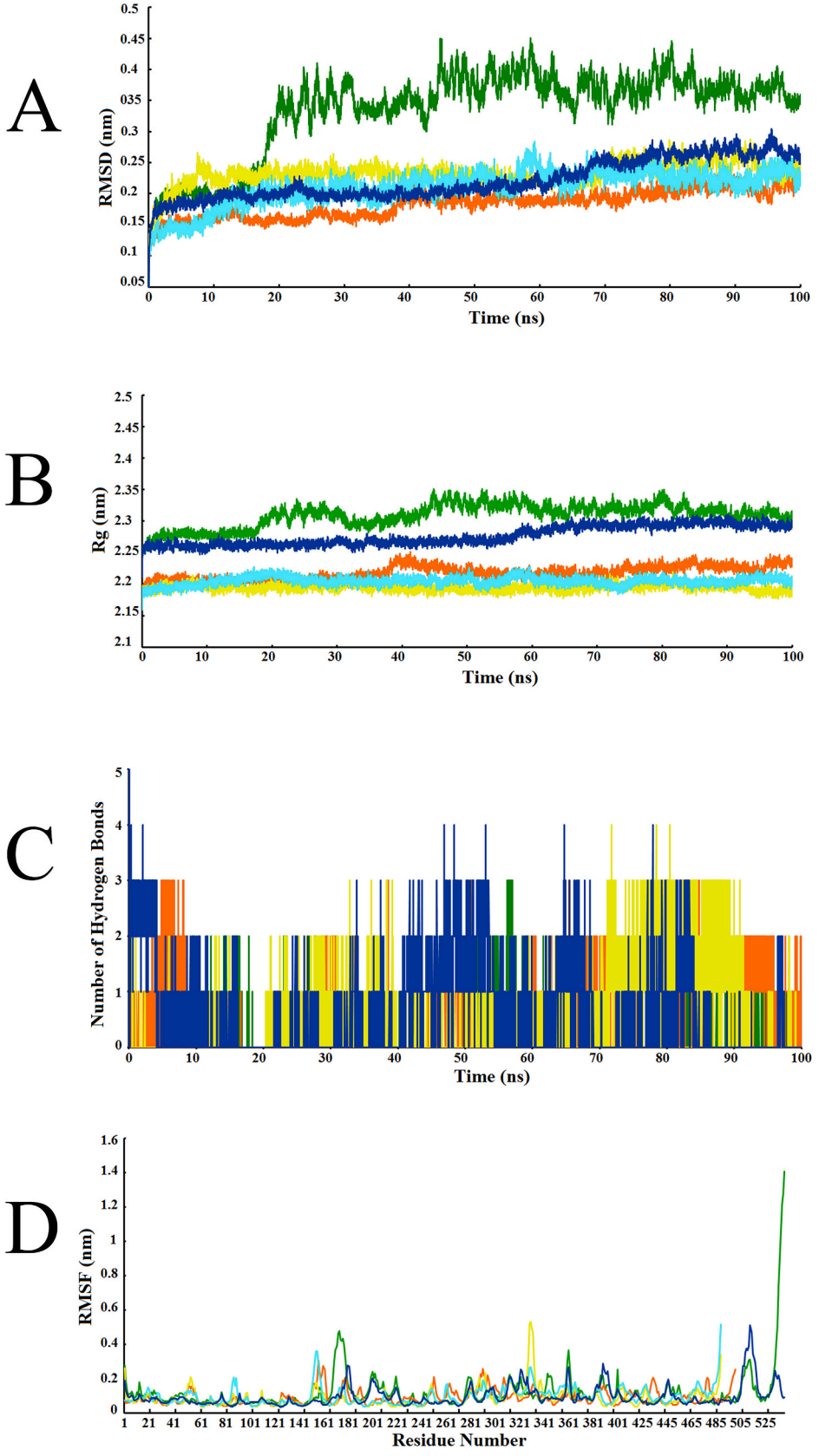

Fig. 5. Comparison of MD simulations results. (A) RMSD plots of the selected Lac/BPs complexes during 100 ns of simulations. (B) Rg plots of the selected Lac/BPs complexes during MD simulations. (C) The number of H-bonds between selected Lac and BPs. (D) RMSF of backbone Ca atoms of the complexes plotted versus residue number in the sequence. In all plots, Lac's *Botrytis aclada*/BPA, Lac's *Trametes hirsuta*/BPAF, Lac's *Rigidoporus microporus*/BPE, Lac'Rigidoporus microporus/BPF, and Lac's Botrytis aclada/BPS complexes are indicated as green, orange, yellow, cyan, and blue, respectively.

3.6. Binding free energy calculations

Binding free energy calculations of complexes were performed for the last 50 ns of the simulations. The results of the calculations are summarized in Table 5. The results reveal that the complexes of Lac's *Trametes hirsuta* with BPAF (−21.83 kJ/mol) and Lac's *Rigidoporus microporus* with BPE (−17.15 kJ/mol) had the highest binding free energy, this energy primarily driven by strong van der Waals interactions. However, the complexes of Lac's *Botrytis aclada* with BPA and Lac's *Rigidoporus microporus* with BPF showed significant binding energies of −12.33 and − 11.02 kJ/mol, respectively. In contrast, Lac's *Botrytis aclada* with BPS exhibited the lowest binding energy (−3.24 kJ/mol). MM/PBSA analysis of the final 50 ns simulation trajectories, including averages and standard deviations, indicated that while van der Waals interactions play a vital role in ligand binding, electrostatic interactions are equally crucial for complex stabilization.

3.7. Per-residue decomposition energy calculations

In this step, the MM/PBSA calculations were performed to analyze the decompose the energetic contributions of key residues in the interaction between selected Lac enzymes and BP compounds. The analysis focused on the last 50 ns of simulations to ensure equilibration of the systems. The results showed that the binding of BPA to Lac's *Botrytis aclada* was primarily driven by van der Waals interactions, with minor electrostatic contributions. Residues Ala184, Pro185, Ser298, and Thr299 showed notable involvement in the interaction. While, the BPS binding to Lac's *Botrytis aclada* involved a more significant number of residues compared to BPA and distributed energetic profile across several residues, including Gly183, Ala184, Pro185, Asp236, Cys297, Ser298, Thr299, Phe365, Trp367, Phe422, Ile424, and His494. Asp236 residues displayed a notable electrostatic contribution. Similar to the other ligands, a complex interplay of van der Waals, electrostatic, and polar solvation contributions was observed.

Also, the binding of BPFA to Lac's *Trametes hirsuta* exhibited that Gly164, Pro391, Gly392, and Ala393 residues contributed significantly to the binding free energy, with a mix of favorable van der Waals and electrostatic interactions. However, substantial polar solvation penalties were also observed, partially offsetting the favorable interactions. This suggests a significant energetic cost of desolvating these residues upon ligand binding. In the binding of BPE to Lac's *Rigidoporus microporus*, Arg336 residue showed the largest contribution to binding, characterized by substantial electrostatic interactions. Other key residues include Phe211, Pro212, Asn213, Ser269, Asn270, Phe343, Gly394, Asn395, His396, Ile454, and His457. Similar to BPE, the Lac's *Rigidoporus microporus*/BPF complex engaged multiple residues in the binding interface. Arg336 residue also played a crucial role in the binding BPF, exhibiting a similar profile of strong but fluctuating electrostatic interactions. Asn395 displayed considerable involvement, with a combination of van der Waals and electrostatic interactions and polar solvation penalties. Other contributing residues included Phe211, Pro212, Asn213, Phe244, Ser269, Asn270, Gly394, His396, Ile454, and His457. Overall, van der Waals interactions play a significant role in all complexes; the relative contributions of electrostatic and solvation terms vary significantly among the selected BP compounds.

4. Discussion

4.1. In silico screening of fungal Lac enzymes predicted effective bioremediation candidates for BP compounds

In this study, the Lac enzymes of thirteen fungal species were selected. A multiple sequence alignment was then performed between the amino acid sequences of the selected Lac enzymes to identify the residues involved in the active sites (Supplementary Fig. S1). Molecular docking was subsequently performed to investigate binding affinity and key interacting residues between the selected Lac enzymes and BP compounds. The results of molecular docking showed that selected Lac enzymes had a binding affinity of more than −5 kcal/mol with BP compounds (Table 2). The screening was carried out to identify the highest binding affinity; however, Lac's *Botrytis aclada* with BPA and BPS (−7.8 and − 7.7 kcal/mol, respectively), Lac's *Trametes hirsuta* with BPAF (−8.5 kcal/mol), and Lac's *Rigidoporus microporus* with BPE and BPF (−8.1 and − 7.8 kcal/mol, respectively) had the highest binding affinity than other selected Lac's fungal. In this regard, Liu Hongyan et al. predicted that the binding affinity of Lac enzyme from *Trametes versicolor* to BPA was −7.25 kcal/mol, while our study showed a comparable value (−7.5 kcal/mol). (Table 2). Also, they reported this enzyme degraded BPA with 97.68 % efficiency under optimized conditions (44.6 °C, pH 5.20, 5 mg/L BPA) [31]. Therefore, these experimental degradation rates (in vitro) confirm that molecular docking reliably identifies highly active Lac enzymes for the degradation of BP compounds. Furthermore, it is likely that enzymes with more negative binding affinity energies (e.g., Lac's *Trametes hirsuta* /BPAF and *Lac's Rigidoporus microporus*/BPE complexes with affinity −8.5 kcal/mol and − 8.1 kcal/mol, respectively) have higher degradation rates in vitro assays.

Also, Zhimin Zhou et al investigated the binding affinity between aflatoxin B1 (AFB_1) and the catalytic cavity of Lac's *Cerrena unicolor* by integrated in silico mutagenesis and in vitro validation. Their study showed that the computationally predicted high affinity binding and strong molecular interactions correlate with the experimentally observed degradation of AFB_1. They reported that variants with optimized substrate binding (e.g., Asn336Arg/Val391Iis) demonstrated increased efficiency in AFB_1 degradation, confirming the hypotheses derived from docking studies. These findings highlight the significant role of structure-function relationships in fungal Lac for the degradation of toxic compounds. Likewise, this consistency justifies the use of docking as a low cost in pre-experimental screening tool and accelerates bioremediation research for the rational design of biocatalysts and

Table 5
Evaluation of the binding free energies (kJ/mol) and energy BP components in the complexes using MM/PBSA.

Ligand	ΔE_{vdW}[a]	ΔE_{ele}[b]	ΔG_{PB}[c]	ΔG_{SA}[d]	ΔE_{gas}[e]	ΔG_{solv}[f]	ΔG_{bind}[g]
BPA	−15.36 ± 1.29	−3.1 ± 0.53	8.06 ± 0.15	−1.92 ± 0.21	−18.47 ± 1.39	6.14 ± 0.26	−12.33 ± 1.42
BPFA	−24.65 ± 2.02	−9.9 ± 1.48	16.38 ± 0.16	−3.67 ± 0.01	−34.54 ± 2.51	12.71 ± 0.16	−21.83 ± 2.51
BPE	−17.26 ± 1.18	−16.18 ± 0.3	18.82 ± 0.14	−2.54 ± 0.01	−33.44 ± 1.22	16.28 ± 0.15	−17.15 ± 1.23
BPF	−14.48 ± 0.18	−3.64 ± 0.74	9.05 ± 0.31	−1.95 ± 0.15	−18.12 ± 0.76	7.11 ± 0.34	−11.02 ± 0.84
BPS	−6.49 ± 0.29	−9.42 ± 2.73	13.61 ± 0.3	−0.94 ± 0.24	−15.91 ± 2.74	12.66 ± 0.38	−3.24 ± 2.77

[a] van der Waals interaction energy (ΔE_{vdW}).
[b] Electrostatic interaction energy (ΔE_{ele}).
[c] Polar solvation energy (ΔG_{PB}).
[d] Nonpolar solvation energy (ΔG_{SA}).
[e] Gas-phase interaction energy (ΔE_{gas}).
[f] Solvation free energy (ΔG_{solv}).
[g] Total binding free energy (ΔG_{bind}).

bioengineering strategies.

4.2. Molecular docking reveals key interactions in Lac/BP complexes

It is well approved that the most common atomic interactions between proteins and ligands are hydrogen bonding and hydrophobic interactions; of course, hydrophobic interactions are the main driving force in protein–ligand binding (57, 58). Also, investigations have revealed that Lac's affinity to substrates depends on hydrogen bond formation. Therefore, the enthalpic contribution of these hydrogen bonds could enhance enzyme-substrate binding affinity, potentially leading to more efficient degradation [51–53]. In this regard, the detailed analysis of interactions between the active center residues of the selected Lac enzymes and the selected BP compounds was discovered that the most significant interactions were hydrophobic. As illustrated in Fig. 3, van der Waals bonds and Pi–alkyl interactions, which are categorized as hydrophobic, play a crucial role in the binding of the selected compounds to Lac enzymes. Additionally, hydrogen bonds significantly contribute to the formation of Lac/BPs complexes. The significant Lac's *Trametes hirsuta* residues involved in these interactions were Gly164, Asn206, Asn264, Phe265, Pro391, Gly392, Ala393, Pro394, His454, Ile455, His458 residues. Also, the key residues of Lac's *Rigidoporus microporus* consist of Ala166, Phe211, Pro212, Asn213, Ser269, Asn270, Arg336, Gly394, Asn395, Pro397, His453, Ile454, Asp455, Trp456, and His457 residues involved in these interactions. Whereas, the key residues of Lac's *Botrytis aclada* involved in hydrophobic and hydrogen interactions were Gly183, Ala184, Pro185, Thr296, Cyc297, Ser298, Thr299, Phe422, Phe365, Trp367, Phe422, Ile424, Ala492, Trp493, and His494 residues.

On the other hand, the structure of BP compounds is characterized by two hydroxyl groups (-OH) attached to two phenolic rings. The variation in BP compound structures depends on the bridging group that connects the two hydroxyphenyl groups. For example, the bridging groups in BPA, BPAF, BPE, BPF, and BPS include two methyl (-CH3-) groups, two trifluoromethyl (-CF3-) groups, an ethylidene (CH3C(H)=) group, a methylene (-CH2-) group, and a sulfone (SO2) group, respectively, that connect the two phenolic rings [26,54]. These structural differences lead to variations in their physicochemical properties, as well as their applications.

Although, the most of interactions showed between the selected active site residues of Lac enzymes and the hydroxyphenyl groups of selected BP compounds, the -CF3- groups of BPAF interestingly interacted with selected active site residues of Lac enzymes. As shown in Fig. 3, the -CF3- groups of BPAF interacted with Lac's *Trametes hirsuta* through a hydrogen bond with Gly392, one pi-alkyl bond with Phe265, and one halogen bond with Ala393. Also, Lac's *Rigidoporus microporus* interacted with the -CF3- groups of BPAF via van der Waals bonds with His457. It also forms one pi-alkyl bond with His457 and two halogen bonds with Gly394. Moreover, the Lac's *Botrytis aclada* interacted with the -CF3- groups of BPAF through a halogen bond with Gly183 and pi-alkyl bonds with Phe365, and Phe422. Consequently, these Lac enzymes had significant interactions with -CF3- groups of BPAF compared to the bridging group at the selected BPs.

Interestingly, S. Alapour et al. reported that the fluorine atoms in the compounds play an important role in both intermolecular and intramolecular non-covalent interactions. These atoms can enhance the binding affinity of compounds to the target protein because they are the most electronegative elements and even can influence the polarity of other groups within the compound [35,55]. In this regard, the presence of fluorine atoms in BPAF's trifluoromethyl (-CF_3-) groups can create unique electronic effects that enhance Lac binding and degradation efficiency.

In Fig. 3 can see that the Lac's *Trametes hirsute*/BPAF complex, the trifluoromethyl (-CF_3-) groups showed non-conventional hydrogen bonds (C-H···F-C) with Gly392 residue. Also, the BPAF showed halogen bonds with key residues of the selected Lac enzyme. However, Shuiqin Jiang et al. demonstrated that halogen bonding significantly influences the substrate binding conformation. They reported that similar to hydrogen bonds and electrostatic interactions, halogen bonds can play an important role in protein-ligand complexes [56].

On the other hand, extensive studies have shown that methyl (-CH_3-) groups significantly influence the biological activity and binding affinity of compounds by increasing their hydrophobicity, thereby enhancing their propensity to bind to proteins [35]. Our results also highlighted the significant role of methyl (-CH_3-) groups in modulating molecular interactions, particularly in BPAF and BPE.

4.3. Lac/BP complexes were stable during MD simulations

RMSD analysis revealed stable conformational behavior in all Lac/BP complexes throughout the 100 ns simulations, confirming strong enzyme-compound interactions. However, the RMSD values for the complexes of Lac's *Trametes hirsuta* with BPAF remained less than 0.22 nm; also, Lac's *Rigidoporus microporus* with BPE and BPF and Lac's *Botrytis aclada* with BPS remained less than 0.28 nm as well as the RMSD values of these complexes were approximately stable throughout the simulation periods. All the same time, the complex of Lac's *Botrytis aclada* with BPA displayed the highest fluctuation of RMSD plot than other complexes during the MD simulations (Fig. 5). Likewise, Lac's *Trametes hirsuta* with BPAF showed the lowest RMSD value.

Also, the result of the Rg value for the complex of Lac's *Botrytis aclada* with BPA showed highest Rg value and most significant fluctuations. In contrast, the complex of Lac's *Botrytis aclada* with BPS also exhibited approximately a high Rg value, but it remained remarkably stable in the 100 ns. Other complexes displayed lower Rg values and notable stability during the simulation.

The H-bond analysis showed that the average number of hydrogen bonds during the simulation was two H-bonds, indicating that the protein-ligand complexes are stabilized after the initial equilibration. However, the fluctuations around the average value are noticeable, indicating the transient nature of some hydrogen bonds.

Additionally, the RMSF plot represented that the complex of Lac's *Botrytis aclada* with BPA and BPS had slight fluctuation in some regions, this is particularly pronounced for residues 160–180 and 505–525 in the C-terminal tail, respectively. In the complex of Lac's *Rigidoporus microporus* with BPE and BPF slightly increased flexibility around residues 325–336 and 150–163, respectively; also, in the C-terminal tail of Lac's *Rigidoporus microporus*. Therefore, it can be suggested slightly increased flexibility in these regens owing to presence of these BP compounds. Whereas, Lac's *Trametes hirsuta* with BPAF showed the lowest fluctuation in 100 ns simulations than other complexes.

Furthermore, based on the binding free energy of complexes Lac's *Trametes hirsuta*/BPAF (−21.83 kJ/mol), Lac's *Rigidoporus microporus*/BPE (−17.15 kJ/mol), Lac's *Botrytis aclada*/BPA (−12.33 kJ/mol), Lac's *Rigidoporus microporus*/BPF (−11.02 kJ/mol), and Lac's *Botrytis aclada*/BPS (−3.24 kJ/mol), it was found that BPAF and BPE had significantly favorable interactions with Lac's *Trametes hirsuta* and *Rigidoporus microporus*, respectively. However, these complexes had high binding affinity (−8.5 and − 8.1 kcal/mol, respectively) and high stability throughout the 100 ns simulations.

These results align with molecular docking finding, where Lac's *Trametes hirsute*/BPAF complex (bearing –CF_3- and –CH_3- groups) and Lac's *Rigidoporus microporus*/BPE (with –CH_3- groups) exhibited the highest binding affinity (binding affinity; −8.5 and-8.1 Kcal/mol, and binding free energies; −21.83 and − 17. 15 kJ/mol, respectively) and stability (lowest RMSD). These findings underscore the affinity of Lac's *Trametes hirsute* and Lac's *Rigidoporus microporus* for fluorine atoms and methyl groups of BPAF and BPE, respectively. Therefore, Lac's *Trametes hirsuta* and *Rigidoporus microporus* can be potential candidates for designing systems to degrade BP compounds, specially BPAF and BPE.

5. Conclusion

Bisphenol A and its derivatives pose significant environmental and health challenges, particularly aquatic animals and humans. This study employed computational approaches — molecular docking and MD simulation — to evaluate the bioremediation of various Lac enzymes from thirteen fungal species against BP compounds (BPA, BPAF, BPE, BPF, and BPS). The findings revealed that the Lac enzyme of *Trametes hirsute*, *Rigidoporus microporu*, and *Botrytis aclada*, exhibited the highest binding affinities and stability with BPAF, BPE/BPF, and BPA/BPS, respectively. Additionally, this study provided a detailed analysis of the interactions between selected Lac enzymes and BP compounds, identifying key residues for binding.

The novelty of this study is in its comparative approach, exploring the interactions between BP compounds and various fungal Lac enzymes, rather than focusing primarily on the well-characterized Lac*'s Trametes versicolor*. Also, these structural insights at the atomic levels enhance our understanding of the efficiency of Lac/BP compound interactions in degradation and highlight the potential of understudied fungal Lac enzymes. Furthermore, the findings establish a theoretical foundation for developing more efficient enzymatic degradation systems. Although experimental validation is required to confirm the computational predictions, these results can significantly inform and optimize future experimental designs, thereby saving time and resources.

5.1. Limitations

This study represents the initial phase of a broader bioremediation project. We acknowledge that while the computational findings presented here provide valuable insights into the molecular interactions between fungal laccases and bisphenol derivatives, experimental validation is essential to confirm these predictions. Therefore, the top-performing Lac/BP complexes identified in this in silico screening will be subjected to thorough in vitro investigations in future work, including enzyme kinetics assays and degradation efficiency measurements. These upcoming experiments are part of our ongoing research and were designed following the computational prioritization provided in this study.

Supplementary data to this article can be found online at https://doi.org/10.1016/j.ijbiomac.2025.145658.

CRediT authorship contribution statement

Reyhaneh Kalhor: Writing – original draft, Visualization, Validation, Supervision, Methodology, Investigation, Formal analysis, Data curation, Conceptualization. **Mahdieh Ameri Shah Reza:** Writing – review & editing, Methodology, Formal analysis, Data curation, Conceptualization. **Rahim Aali:** Writing – review & editing, Funding acquisition, Formal analysis, Data curation, Conceptualization. **Hoda Abolhasani:** Writing – review & editing, Methodology, Formal analysis, Data curation. **Mohammad Hossein Mokhtarian:** Writing – review & editing, Visualization, Methodology. **Hourieh Kalhor:** Writing – review & editing, Writing – original draft, Visualization, Validation, Supervision, Software, Project administration, Methodology, Investigation, Funding acquisition, Formal analysis, Data curation, Conceptualization.

Funding/Support

This study was supported by the Cellular and Molecular Research Center of Qom University of Medical Sciences, Qom, Iran (grant number: 1746, 2024).

Declaration of competing interest

The authors declare that they have no known competing financial interests or personal relationships that could have appeared to influence the work reported in this paper.

Acknowledgements

The authors would like to express their sincere gratitude to the Qom University of Medical Sciences and Health Services for their financial support. We are also grateful to the Ethics Committee of Qom University of Medical Sciences for their approval of this study (Ethics code: IR.MUQ.MEDICINE.REC.1402.228).

Data availability

Data will be made available on request.

References

[1] K.E. Pelch, J.A. Wignall, A.E. Goldstone, P.K. Ross, R.B. Blain, A.J. Shapiro, S. D. Holmgren, J.-H. Hsieh, D. Svoboda, S.S. Auerbach, NTP Research Report on Biological Activity of Bisphenol a (BPA) Structural Analogues and Functional Alternatives: Research Report 4, 2020.
[2] Y. Li, L. Chen, Y. Sun, R. Wang, B. Zhao, T. Jing, Exploring the effect of surfactants on the interaction between laccase and bisphenol a by molecular docking, molecular dynamics, and energy calculations, J. Mol. Liq. 382 (2023) 121928.
[3] L. Xie, B. Huang, X. Zhao, N. Zhu, Exploring the mechanisms underlying effects of bisphenol a on cardiovascular disease by network toxicology and molecular docking, Heliyon 10 (10) (2024).
[4] M. Murata, J.-H. Kang, Bisphenol a (BPA) and cell signaling pathways, Biotechnol. Adv. 36 (1) (2018) 311–327.
[5] L.M. Vermeer, E. Gregory, M.K. Winter, K.E. McCarson, N.E. Berman, Exposure to bisphenol A exacerbates migraine-like behaviors in a multibehavior model of rat migraine, Toxicological Sciences 137 (2) (2014) 416–427.
[6] Z. Wang, H. Liu, S. Liu, Low-dose bisphenol a exposure: a seemingly instigating carcinogenic effect on breast cancer, Adv. Sci. 4 (2) (2017), 1600248.
[7] M. Ramadan, B. Cooper, N.G. Posnack, Bisphenols and phthalates: plastic chemical exposures can contribute to adverse cardiovascular health outcomes, Birth Defects Research 112 (17) (2020) 1362–1385.
[8] R. Chianese, J. Troisi, S. Richards, M. Scafuro, S. Fasano, M. Guida, R. Pierantoni, R. Meccariello, Bisphenol a in reproduction: epigenetic effects, Curr. Med. Chem. 25 (6) (2018) 748–770.
[9] F. Cariati, N. D'Uonno, F. Borrillo, S. Iervolino, G. Galdiero, R. Tomaiuolo, Bisphenol a: an emerging threat to male fertility, Reprod. Biol. Endocrinol. 17 (2019) 1–8.
[10] R. Frankowski, A. Zgoła-Grześkowiak, W. Smułek, T. Grześkowiak, Removal of bisphenol a and its potential substitutes by biodegradation, Appl. Biochem. Biotechnol. 191 (2020) 1100–1110.
[11] J. Trivedi, U. Chhaya, Bioremediation of bisphenol A found in industrial wastewater using Trametes versicolor (TV) laccase nanoemulsion-based bead organogel in packed bed reactor, Water Environ. Res. 94 (10) (2022) e10786.
[12] J. Torres-García, M. Ahuactzin-Pérez, F. Fernández, D.V. Cortés-Espinosa, Bisphenol A in the environment and recent advances in biodegradation by fungi, Chemosphere 303 (2022) 134940.
[13] M. Bilal, T. Rasheed, F. Nabeel, H.M. Iqbal, Y. Zhao, Hazardous contaminants in the environment and their laccase-assisted degradation–a review, J. Environ. Manage. 234 (2019) 253–264.
[14] P. Bhardwaj, N. Kaur, M. Selvaraj, H.A. Ghramh, B.M. Al-Shehri, G. Singh, S. K. Arya, K. Bhatt, S. Ghotekar, R. Mani, Laccase-assisted degradation of emerging recalcitrant compounds–a review, Bioresour. Technol. 364 (2022) 128031.
[15] S.G. Ramakrishnan, M. Sivaramakrishnan, D. Chenthamara, R. Kothandan, S. Krishnaswami, S. Subramaniam, Modelling, docking and simulation analysis of bisphenol a interaction with laccase from Trichoderma, Bioinformation 16 (4) (2020) 323.
[16] T. Bertrand, C. Jolivalt, P. Briozzo, E. Caminade, N. Joly, C. Madzak, C. Mougin, Crystal structure of a four-copper laccase complexed with an arylamine: insights into substrate recognition and correlation with kinetics, Biochemistry 41 (23) (2002) 7325–7333.
[17] M. Awasthi, N. Jaiswal, S. Singh, V.P. Pandey, U.N. Dwivedi, Molecular docking and dynamics simulation analyses unraveling the differential enzymatic catalysis by plant and fungal laccases with respect to lignin biosynthesis and degradation, Journal of Biomolecular Structure and Dynamics 33 (9) (2015) 1835–1849.
[18] M. Mahuri, M. Paul, S.K. Sahu, H. Thatoi, In silico homology modeling, docking and sequence analysis of some bacterial laccases to unravel enzymatic specificity towards lignin biodegradation, J. Biomol. Struct. Dyn. 41 (12) (2023) 5757–5775.
[19] K. Chakraborty, K.K. Hazarika, S.K. Sil, A. Ghosh, Studies on substrate specificity of the enzyme laccase: an in-silico approach, Trends Carbohydr. Res. 14 (3) (2022).
[20] M. Inoue, Y. Masuda, F. Okada, A. Sakurai, I. Takahashi, M. Sakakibara, Degradation of bisphenol a using sonochemical reactions, Water Res. 42 (6–7) (2008) 1379–1386.
[21] A. Garg, T. Singhania, A. Singh, S. Sharma, S. Rani, A. Neogy, S.R. Yadav, V. K. Sangal, N. Garg, Photocatalytic degradation of bisphenol-a using N, co codoped TiO2 catalyst under solar light, Sci. Rep. 9 (1) (2019) 765.

[22] Z. Jiao, L. Chen, G. Zhou, H. Gong, X. Zhang, Y. Liu, X. Gao, Degradation of bisphenol a by CeCu oxide catalyst in catalytic wet peroxide oxidation: efficiency, stability, and mechanism, Int. J. Environ. Res. Public Health 16 (23) (2019) 4675.
[23] M.J. dos Santos Costa, J.V.S. Araújo, J.K.L. Moura, L.H. da Silva Moreno, P. A. Pereira, R. da Silva Santos, C.V.R. Moura, A brief review of detection and removal of bisphenol A in aqueous media, Water, Air, & Soil Pollution 233 (9) (2022) 362.
[24] E.J. Eio, M. Kawai, K. Tsuchiya, S. Yamamoto, T. Toda, Biodegradation of bisphenol A by bacterial consortia, Int. Biodeter. Biodegr. 96 (2014) 166–173.
[25] Y. Han, H. Dai, X. Rong, H. Jiang, Y. Xue, Research progress of methods for degradation of bisphenol a, Molecules 28 (24) (2023) 8028.
[26] M. Kolb, V. Sieber, M. Amann, M. Faulstich, D. Schieder, Removal of monomer delignification products by laccase from Trametes versicolor, Bioresour. Technol. 104 (2012) 298–304.
[27] M. Alshabib, S.A. Onaizi, Enzymatic remediation of bisphenol A from wastewaters: effects of biosurfactant, anionic, cationic, nonionic, and polymeric additives, Water Air Soil Pollut. 231 (2020) 1–13.
[28] D. Daâssi, A. Prieto, H. Zouari-Mechichi, M.J. Martínez, M. Nasri, T. Mechichi, Degradation of bisphenol a by different fungal laccases and identification of its degradation products, Int. Biodeter. Biodegr. 110 (2016) 181–188.
[29] S. Kurniawati, J.A. Nicell, Characterization of Trametes versicolor laccase for the transformation of aqueous phenol, Bioresour. Technol. 99 (16) (2008) 7825–7834.
[30] R. Díaz, G. Díaz-Godínez, M.A. Anducho-Reyes, Y. Mercado-Flores, L.D. Herrera-Zúñiga, In silico design of laccase thermostable mutants from Lacc 6 of Pleurotus ostreatus, Front. Microbiol. 9 (2018) 2743.
[31] L. Hongyan, Z. Zexiong, X. Shiwei, X. He, Z. Yinian, L. Haiyun, Y. Zhongsheng, Study on transformation and degradation of bisphenol a by Trametes versicolor laccase and simulation of molecular docking, Chemosphere 224 (2019) 743–750.
[32] V. Vijayalakshmi, P. Senthilkumar, K. Mophin-Kani, S. Sivamani, N. Sivarajasekar, S. Vasantharaj, Bio-degradation of bisphenol A by Pseudomonas aeruginosa PAb1 isolated from effluent of thermal paper industry: kinetic modeling and process optimization, Journal of Radiation Research and Applied Sciences 11 (1) (2018) 56–65.
[33] R. Huey, G.M. Morris, S. Forli, Using AutoDock 4 and AutoDock vina with AutoDockTools: a tutorial, The Scripps Research Institute Molecular Graphics Laboratory 10550 (92037) (2012) 1000.
[34] S. Fereshteh, N. Noori Goodarzi, H. Kalhor, H. Rahimi, S.M. Barzi, F. Badmasti, Identification of putative drug targets in highly resistant gram-negative bacteria; and drug discovery against Glycyl-tRNA synthetase as a new target, Bioinformatics and Biology Insights 17 (2023), 11779322231152980.
[35] H. Kalhor, H. Rahimi, M.R.A. Eidgahi, L. Teimoori-Toolabi, Novel small molecules against two binding sites of Wnt2 protein as potential drug candidates for colorectal cancer: a structure based virtual screening approach, Iranian Journal of Pharmaceutical Research 19 (2) (2020) 160.
[36] C. Martínez-Sotres, J.G. Rutiaga-Quiñones, R. Herrera-Bucio, M. Gallo, P. López-Albarrán, Molecular docking insights into the inhibition of laccase activity by medicarpin, Wood Sci. Technol. 49 (2015) 857–868.
[37] J. Kallio, S. Auer, J. Jänis, M. Andberg, K. Kruus, J. Rouvinen, A. Koivula, N. Hakulinen, Structure–function studies of a Melanocarpus albomyces laccase suggest a pathway for oxidation of phenolic compounds, J. Mol. Biol. 392 (4) (2009) 895–909.
[38] G. Ranimol, C. Devipriya, S. Sunkar, Docking and Molecular Dynamics Simulation Studies for the Evaluation of Laccase Mediated Biodegradation of Triclosan, Conference BioSangam 2022: Emerging Trends in BIOTECHNOLOGY (BIOSANGAM 2022), Atlantis Press, 2022, pp. 205–213.
[39] N.M. O'Boyle, M. Banck, C.A. James, C. Morley, T. Vandermeersch, G. R. Hutchison, Open babel: an open chemical toolbox, J. Chem. 3 (2011) 1–14.
[40] O. Trott, A.J. Olson, AutoDock Vina: improving the speed and accuracy of docking with a new scoring function, efficient optimization, and multithreading, J. Comput. Chem. 31 (2) (2010) 455–461.
[41] W.L. DeLano, ymol: an open-source molecular graphics tool, CCP4 Newsl, Protein Crystallogr 40 (1) (2002) 82–92.
[42] D. Studio, Discovery studio, Accelrys 2.1 (2008) 420.
[43] T. Sander, J. Freyss, M. Von Korff, C. Rufener, DataWarrior: an open-source program for chemistry aware data visualization and analysis, J. Chem. Inf. Model. 55 (2) (2015) 460–473.
[44] V. Zoete, M.A. Cuendet, A. Grosdidier, O. Michielin, SwissParam: a fast force field generation tool for small organic molecules, J. Comput. Chem. 32 (11) (2011) 2359–2368.
[45] N. Homeyer, H. Gohlke, Free energy calculations by the molecular mechanics Poisson−Boltzmann surface area method, Mol. Inf. 31 (2) (2012) 114–122.
[46] F. Darvishi, E. Beiranvand, H. Kalhor, B. Shahbazi, L. Mafakher, Homology modeling and molecular docking studies to decrease glutamine affinity of Yarrowia lipolytica L-asparaginase, Int. J. Biol. Macromol. 263 (2024) 130312.
[47] H. Kalhor, S. Sadeghi, H. Abolhasani, R. Kalhor, H. Rahimi, Repurposing of the approved small molecule drugs in order to inhibit SARS-CoV-2 S protein and human ACE2 interaction through virtual screening approaches, Journal of Biomolecular Structure and Dynamics 40 (3) (2022) 1299–1315.
[48] H. Kalhor, S. Sadeghi, M. Marashiyan, R. Kalhor, S. Aghaei Gharehbolagh, M. R. Akbari Eidgahi, H. Rahimi, Identification of new DNA gyrase inhibitors based on bioactive compounds from streptomyces: structure-based virtual screening and molecular dynamics simulations approaches, Journal of Biomolecular Structure and Dynamics 38 (3) (2020) 791–806.
[49] H. Kalhor, H. Abolhasani, R. Kalhor, T. Komeili Movahhed, H. Rahimi, Interactions of heparin derivatives with recombinant human keratinocyte growth factor: structural stability and bioactivity effect study, Proteins: Struct., Funct., Bioinf. 91 (4) (2023) 542–554.
[50] H. Kalhor, M.H. Mokhtarian, H. Rahimi, B. Shahbazi, R. Kalhor, T.K. Movahed, H. Abolhasani, Predictive Insights Into Bioactive Compounds from Streptomyces as Inhibitors of SARS-CoV-2 Mutant Strains by Receptor Binding Domain: Molecular Docking and Dynamics Simulation Approaches, IJ Pharmaceutical Research 23(1).
[51] L. Dellafiora, G. Galaverna, M. Reverberi, C. Dall'Asta, Degradation of aflatoxins by means of laccases from Trametes versicolor: an in silico insight, Toxins 9 (1) (2017) 17.
[52] M. Xia, J. Zheng, S. Chen, Y. Tang, S. Wang, Z. Ji, T. Hao, H. Li, L. Li, R.-S. Ge, Bisphenol a alternatives suppress human and rat aromatase activity: QSAR structure-activity relationship and in silico docking analysis, Food Chem. Toxicol. 183 (2024) 114257.
[53] Z. Zhou, R. Li, T.B. Ng, F. Huang, X. Ye, Considerations regarding affinity determinants for aflatoxin B1 in binding cavity of fungal laccase based on in silico mutational and in vitro verification studies, Ecotoxicol. Environ. Saf. 234 (2022) 113412.
[54] R.K. Pathak, D.-W. Jung, S.-H. Shin, B.-Y. Ryu, H.-S. Lee, J.-M. Kim, Deciphering the mechanisms and interactions of the endocrine disruptor bisphenol a and its analogs with the androgen receptor, J. Hazard. Mater. 469 (2024) 133935.
[55] S. Alapour, S. Zamisa, J. Silva, C. Alves, B. Omondi, D. Ramjugernath, N. Koorbanally, Investigations into the flexibility of the 3D structure and rigid backbone of quinoline by fluorine addition to enhance its blue emission, CrystEngComm 20 (16) (2018) 2316–2323.
[56] S. Jiang, L. Zhang, D. Cui, Z. Yao, B. Gao, J. Lin, D. Wei, The important role of halogen bond in substrate selectivity of enzymatic catalysis, Sci. Rep. 6 (1) (2016), 34750.